

Lateral coherence properties of broad-area semiconductor quantum well lasers

A. Larsson,^{a)} J. Salzman,^{b)} M. Mittelstein, and A. Yariv
California Institute of Technology, Pasadena, California 91125

(Received 2 January 1986; accepted for publication 11 March 1986)

The lateral coherence of broad-area lasers fabricated from a GaAs/GaAlAs graded index waveguide separate confinement and single quantum well heterostructure grown by molecular-beam epitaxy was investigated. These lasers exhibit a high degree of coherence along the junction plane, thus producing a stable and very narrow far field intensity distribution.

Considerable effort has been invested in the development of semiconductor lasers with a high output power and a narrow beam far field pattern (FFP). Most of these efforts to date were devoted to the development of phase-locked laser arrays.¹⁻⁶ Other approaches to achieve a similar task include unstable resonator semiconductor lasers^{7,8} and lateral gain tailored lasers.⁹ Common to all the above-mentioned approaches is the use of a broad-area geometry, with a proper modulation of the laser cavity in the lateral or in the longitudinal dimension. All the above methods rely on the formation of a modified cavity which has a higher mode selection, thus favoring the oscillation of its fundamental lateral mode. However, none of the investigated solutions is free from saturation effects (spatial hole burning). Therefore, increasing the injection current to several times the threshold current leads to the onset of higher-order modes with the subsequent broadening of the FFP.¹⁰ An additional degree of freedom in the design of high-power semiconductor lasers is the transverse dimension (the layer structure). The advantages of semiconductor lasers with quantum well heterostructures over these with regular double heterostructures have been largely recognized,^{11,12} but the effect of an improved heterostructure on the lateral beam divergence of a broad-area device has not been explored. An indication of the effect of improving the material properties on the beam divergence of a broad-area laser (in this case, a single quantum well, separate confinement heterostructure) was provided by Tsang.¹³ According to his report, a 200- μm -wide laser emitted in a stable, single-lobe far field pattern with a full width at half maximum (FWHM) of 4° . This far field angle is substantially smaller than that of a conventional broad-area laser and it corresponds to a coherence width of $\sim 12\text{--}14\ \mu\text{m}$ which is larger than the width of a typical filament ($\sim 5\ \mu\text{m}$). Moreover, the extremely high stability of the FFP up to injection currents as high as $I = 6.3 \times I_{\text{th}}$, where I_{th} is the threshold current, suggests that this laser is less susceptible to spatial hole burning effects, thus preventing the near field intensity distribution from changing with injection current. In this paper the beam characteristics of a broad-area laser fabricated from a graded index waveguide, separate confinement, single quantum well heterostructure

(GRIN-SCH) are investigated.¹⁴

The wafers for the fabrication of broad-area lasers were grown by molecular-beam epitaxy (MBE) and included a superlattice buffer layer and a GRIN-SCH single quantum well structure as depicted in Fig. 1. A shallow Zn diffusion was performed for improving the formation of an ohmic contact on the upper $p\text{-Ga}_{0.5}\text{Al}_{0.5}\text{As}$ layer, and then lasers 100 μm wide and with different lengths were fabricated by conventional methods. The lasers were tested with 100 ns pulses and low duty cycle.

The (pulsed) threshold current density and differential quantum efficiency are $230\ \text{A}/\text{cm}^2$ and 0.84, respectively, for a 480- μm long cavity.¹⁵ Similar to the case of previously reported lasers made from MBE-grown heterostructures, the near field intensity distribution exhibited a uniformity of $u \approx 0.8$.¹⁶ The high degree of uniformity across the emitting area has a positive effect on increasing the output power at which catastrophic damage occurs, but does not ensure a narrow and stable FFP, because a nearly uniform near field may result from the incoherent superposition of several lateral modes with higher-order modes radiating energy off axis. In most of the tested lasers, the observed FFP is single lobed, near 2° FWHM but in some cases the measured FFP at $I_{\text{th}} < I < 1.2I_{\text{th}}$ is as narrow as 0.8° (Fig. 2).¹⁶

Such a narrow FFP is consistent with operation only in the fundamental lateral mode of the gain-induced 100- μm -wide waveguide, but it would be surprising if this mode oscillated.

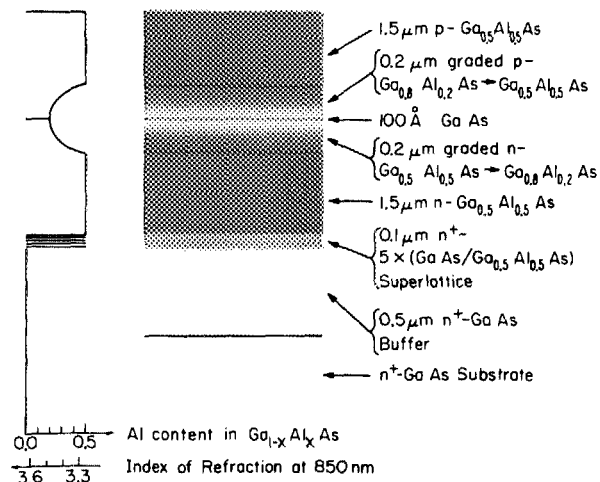


FIG. 1. Single quantum well GRIN-SCH structure with superlattice buffer layer used in this work.

^{a)} On leave from the Department of Electrical Measurements, Chalmers University of Technology, S-41296 Goteborg, Sweden.

^{b)} Present address: Bell Communication Research, Murray Hill, New Jersey 07974.

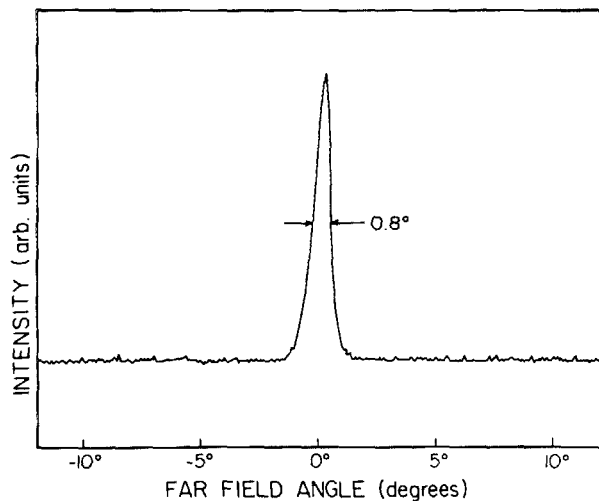


FIG. 2. Far field pattern of the broad-area, single quantum well GRIN-SCH laser for $I = 1.1 \times I_{th}$.

lates while higher-order modes are expected to have higher modal gain.

The measured near field intensity distribution for different values of the injection current is shown in Fig. 3. Note the high stability of this near field with current, and the nearly periodic lateral variations in the intensity, resembling filaments.^{17,18}

Additional information on the emission characteristics was provided by measuring the spatial coherence between different points at the laser near field. This was performed by imaging the laser near field on the plane of a double slit with adjustable separation, and observing the visibility of the interference fringes produced by the light transmitted through the two slits (Young experiment).¹⁹ A typical interference pattern from two points $50 \mu\text{m}$ apart is shown in Fig. 4, with a fringe visibility function of 67%. A high degree of spatial coherence was measured up to lateral separations of $80 \mu\text{m}$, but some regions of the laser near field exhibited lower coherence even at a small slit separation. In many lasers, the measured lateral coherence was increased with increasing

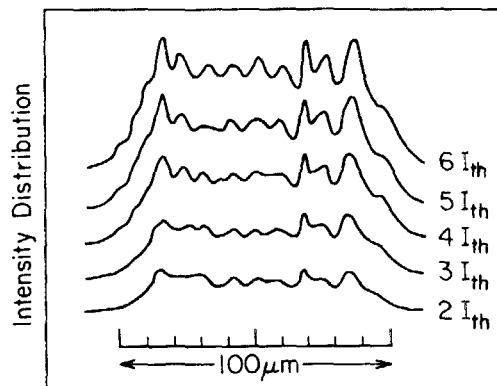


FIG. 3. Near field intensity distribution for different values of the injection current.

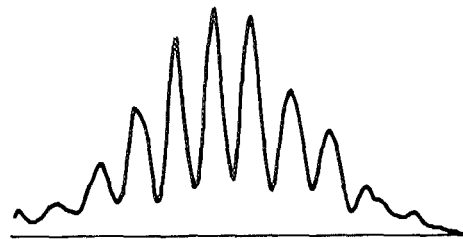


FIG. 4. Interference pattern between two points at the laser facet, $50 \mu\text{m}$ apart.

injection current up to $I \sim 3 \times I_{th}$. At $I = 8 \times I_{th}$ the fringe visibility function degraded considerably. These coherence measurements were performed on a large number of lasers, with very similar results, concluding that several of the “perturbed” lateral modes are oscillating simultaneously, with the more uniformly distributed mode prevailing at higher injection currents. Assuming that each one of the coexisting modes emits with a nearly planar phase front in the on-axis direction, the incoherent superposition of these modes will produce a FFP with an angular width determined by the mode with the smallest lateral extent in the near field.²⁰ In the case of Fig. 2, we conclude that this mode covers at least $70 \mu\text{m}$ out of our $100\text{-}\mu\text{m}$ wide laser. Most of the lasers measured exhibited FFP’s consistent with $30\text{--}40 \mu\text{m}$ of lateral coherence. In Fig. 5 we present a photograph of the spectrally resolved near field spectrum. Different *longitudinal* modes are observed. Lateral modes corresponding to a given longitudinal mode are not resolved in this picture but it seems very likely that three sets of lateral “perturbed” modes are oscillating with one of them (at the bottom of the figure) extending over the whole laser width. We would like to mention that, although the observed FFP is very narrow and stable in most cases, the near field intensity distribution and the regions of lateral coherence vary considerably.

The above-mentioned measurements can be interpreted in a simple way: regenerative self-focusing leads to the formation of filaments, but these filaments tend to be phase locked in the same fashion as semiconductor laser arrays.

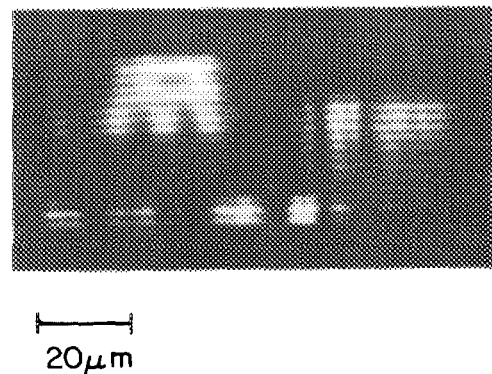


FIG. 5. Spectrally resolved near field intensity distribution for $I = 1.6 \times I_{th}$. The vertical axis corresponds to wavelength and the horizontal axis is the lateral dimension. The longitudinal mode separation is $\Delta\lambda = 2.2 \text{ \AA}$.

These phase-locked filaments are still subject to some degree of randomness and do not always extend over the full laser width. The control of the filaments by very slight changes in the laser geometry in order to produce a stable phase-locked array can be implemented and is the subject of a forthcoming publication.²¹

The last question we would like to address is: why is the filamentary behavior of these lasers so different from that of conventional broad-area double heterostructure lasers? Three reasons contribute to that: (i) the important factor determining the strength of self-focusing is the change in the effective refractive index Δn induced by the injected carriers N at the laser threshold.¹⁷ It has been previously shown that Δn and $\partial n / \partial N$ are drastically reduced in a quantum well structure in comparison to these values in regular double heterostructures.²³ As a result of that, self-focusing is drastically reduced, and the filament effective width is increased. This facilitates the coupling between neighboring filaments. (ii) the extremely high uniformity of the MBE-grown structure results in a nearly uniform gain below threshold. This favors the formation of uniformly distributed, closely spaced filaments. (iii) In conventional lasers, spatial mode instability is related to gain saturation and extra gain present in regions where the oscillating mode has a low intensity. The phase-locked filaments form a "perturbed" mode which is nearly uniform over the laser width and then are expected to be more stable than the unperturbed modes of the waveguide or than isolated filaments. It is worth mentioning that a necessary condition for a uniform, index-guided phased array to lock in phase (and therefore to exhibit a single-lobed FFP) is to have high gain in the regions of low refractive index and vice versa.²² This condition is fulfilled by a self-focused laser in multifilamentary operation.¹⁷

In conclusion, we have shown that broad-area GRIN-SCH lasers can produce a stable, single-lobed, and extremely narrow FFP. The radiation characteristics of these lasers can be explained in terms of phase-locked filaments. Our experimental results suggest that this improved laser heterostructure may result in an optical output power, a far field pattern, and a mode stability comparable to, or better than, that obtained in laser arrays or in other geometrical configurations,

without any lateral modulation in the gain or in the refractive index.

The work described in this paper was performed under a contract with the National Aeronautics and Space Administration (NAS7-918) and under grants from the Office of Naval Research and the Army Research Office. J. Salzman would like to acknowledge the support of the Bantrell postdoctoral Fellowship and the Fullbright Fellowship. The authors would like to thank Y. Arakawa for assistance in the fabrication of the lasers used in this work.

¹D. R. Scifres, R. D. Burnham, and W. Streifer, *Appl. Phys. Lett.* **33**, 1015 (1978).

²D. R. Scifres, W. Streifer, and R. D. Burnham, *IEEE J. Quantum Electron.* **QE-15**, 917 (1979).

³D. E. Ackley and R. W. H. Engleman, *Appl. Phys. Lett.* **39**, 27 (1981).

⁴E. Kapon, J. Katz, C. Lindsey, S. Margalit, and A. Yariv, *Appl. Phys. Lett.* **43**, 421 (1983).

⁵E. Kapon, C. Lindsey, J. Katz, S. Margalit, and A. Yariv, *Appl. Phys. Lett.* **45**, 200 (1984).

⁶H. Temkin, R. A. Logan, and J. P. van der Ziel, *Appl. Phys. Lett.* **46**, 465 (1985).

⁷J. Salzman, T. Venkatesan, R. Lang, M. Mittelstein, and A. Yariv, *Appl. Phys. Lett.* **46**, 218 (1985).

⁸J. Salzman, R. Lang, A. Larsson, and A. Yariv (unpublished).

⁹C. Lindsey, P. Derry, and A. Yariv, *Electron. Lett.* **21**, 671 (1985).

¹⁰K. L. Chen and S. Wong, *Appl. Phys. Lett.* **47**, 555 (1985).

¹¹N. Holonyak, Jr., R. M. Kolbas, R. D. Dupuis, and P. D. Dapkus, *IEEE J. Quantum Electron.* **QE-16**, 170 (1980).

¹²W. T. Tsang, *IEEE J. Quantum Electron.* **QE-20**, 1119 (1984) and references therein.

¹³W. T. Tsang, *Electron. Lett.* **16**, 939 (1980).

¹⁴W. T. Tsang, *Appl. Phys. Lett.* **39**, 134 (1981).

¹⁵A. Larsson, M. Mittelstein, Y. Arakawa, and A. Yariv (unpublished).

¹⁶W. T. Tsang, *Appl. Phys. Lett.* **34**, 473 (1979).

¹⁷G. H. B. Thompson, *Opto-electronics* **4**, 257 (1972).

¹⁸J. Salzman, A. Larsson, and A. Yariv, paper presented at Annual Meeting of the Optical Society of America, Washington, D. C., Oct. 14-18, 1985.

¹⁹M. Mittelstein, J. Salzman, T. Venkatesan, R. Lang, and A. Yariv, *Appl. Phys. Lett.* **46**, 923 (1985).

²⁰The FFP is actually the weighted average of the spatial Fourier transforms of the lateral modes near field, with the intensity of each mode as the weighting factor.

²¹J. Salzman, A. Larsson, and A. Yariv (unpublished).

²²W. Streifer, A. Hardy, and R. D. Burnham, *Electron Lett.* **21**, 118 (1985).

²³N. K. Dutta, N. A. Olsson, and W. T. Tsang, *Appl. Phys. Lett.* **45**, 836 (1984).